Contents lists available at ScienceDirect

Journal of Pharmaceutical Analysis

ORIGINAL ARTICLE

Determination of drug, excipients and coating distribution in pharmaceutical tablets using NIR-CI

Anna Palou[a], Jordi Cruz[b], Marcelo Blanco[a], Jaume Tomàs[c],
Joaquín de los Ríos[c], Manel Alcalà[a,*]

[a]Unitat de Química Analítica, Departament de Química, Facultat de Ciències, Universitat Autònoma de Barcelona, 08193 Bellaterra, Barcelona, Spain
[b]Escola Universitària Salessiana de Sarrià, Passeig Sant Joan Bosco, 74, 08017 Barcelona, Spain
[c]Esteve Farma, c/Sant Martí s/n, 08197 Martorelles, Barcelona, Spain

Abstract   The growing interest of the pharmaceutical industry in Near Infrared-Chemical Imaging (NIR-CI) is a result of its high usefulness for quality control analyses of drugs throughout their production process (particularly of its non-destructive nature and expeditious data acquisition). In this work, the concentration and distribution of the major and minor components of pharmaceutical tablets are determined and the spatial distribution from the internal and external sides has been obtained. In addition, the same NIR-CI allowed the coating thickness and its surface distribution to be quantified. Images were processed to extract the target data and calibration models constructed using the Partial Least Squares (PLS) algorithms. The concentrations of Active Pharmaceutical Ingredient (API) and excipients obtained for uncoated cores were essentially identical to the nominal values of the pharmaceutical formulation. But the predictive ability of the calibration models applied to the coated tablets decreased as the coating thickness increased.

*Corresponding author. Tel./fax: +34 935814899.
E-mail address: manel.alcala@uab.cat (M. Alcalà)

1. Introduction

Near Infrared-Chemical Imaging (NIR-CI) is a technique based on conventional NIR spectroscopy with the added advantage that it affords recording of a large amount of both spectral and spatial information in a single image. While the conventional NIR technique only provides the average spectrum for the surface of each sample, NIR-CI gives one spectrum per pixel in each acquired image and hence much more information about the whole sample surface [1]. The easiness to obtain this information through with NIR-CI has aroused interest in NIR-CI in many fields of study. This is

particularly applicable in the analysis of pharmaceutical products, which is made easy by NIR-CI by virtue of its ability to acquire a vast amount of information in an expeditious manner, all without altering the sample. The increasing interest aroused by NIR-CI in the pharmaceutical field is evident from the variety of studies based on this technique reported in recent years. Such studies include the homogeneity of powder samples [2], particle size determinations [3], product composition [4], the determination of the concentrations and distribution of components in solid tablets [5] and content uniformity [6], among others. Also, the many uses of NIR-CI in the pharmaceutical industry have been the subject of two interesting reviews [1,7].

Film coatings on commercial tablets have been the subject of some study [8,9], but not so much as pharmaceutical components despite their significance. The coating film applied to a drug tablet is primarily intended to improve its esthetics and function. Thus, the coating allows the unpleasant taste of some APIs to be masked and facilitates swallowing of tablets, in addition to preserving their integrity and giving them a uniform appearance. Some coatings, however, are intended to facilitate the controlled or enteric release of the dosage form of a drug [10]. In any case, the exact function of a coating depends largely on its thickness and distribution on the tablet surface. In fact, too thin or too thick a coating can alter the effectiveness of a tablet by making the core more vulnerable to external factors or diminishing the API release rate. Simply measuring the average thickness of the lacquer film on a tablet is inadequate to ensure that the tablet will meet the specifications; rather, this requires obtaining more information about the way the coating is distributed throughout the tablet surface. The capabilities of the NIR-CI technique in this respect make it a suitable choice for quality control in tablet production processes.

However, the vast amount of information contained in a hyperspectral image requires the use of an effective procedure to extract it. In fact, hyperspectral data form a three-way cube that must be unfolded and processed with appropriate two-way multivariate algorithms in order to extract the target information.

In those cases where some components of a pharmaceutical are unknown or a spectrum unavailable, algorithms requiring no calibration set are especially useful; such algorithms include Multivariate Curve Resolution-Alternating Least Squares (MCR-ALS) [11] and its augmented form [12]. However, the process involved in extracting information from chemical images can be slow and cumbersome. One alternative choice in wide use for the quantitative analysis of CI data is Partial Least Squares (PLS) [13]. The Isys software included with the NIR-CI instrument allows the easy application of PLS for a rapid and accurate determination of components distribution in a sample. This algorithm requires a series of data distributed over a wide enough range of specific values of the target property to allow the construction of a suitable calibration model for the samples to be analyzed. Each pixel of the image is assigned to a response matrix based on the similarity of its spectra with those for the pure components [14].

In this work we intend to evaluate the distribution of the components in a tablet and quantify the thickness and surface distribution of the film coating during the development of a new pharmaceutical formulation. Individual calibration models for the components were used to obtain their distribution

map and a calibration model derived from the NIR-CI hyperspectral image was used to establish the distribution map for the coating film.

2. Materials and methods

2.1. Samples

We studied three different types of samples, namely: (a) cores (uncoated tablets), (b) tablets with a coating of variable thickness and (c) tablets with the standard coating. The coated tablets (b) included samples with film thicknesses between $0x$ and $3x$, where x is considered the standard coating thickness of tablets (c).

We consider the coating process is constant and reproducible along time. The standard time encompasses a coating thickness namely x. The double or triple of this standard time are named $2x$ and $3x$. The reference coating thickness has been calculated measuring the approximate tablet surface (1.92 cm^2), the tablet weight difference before and after coating (from 290 mg to 317 mg) and the real density of the coating polymer (1.19 g/cm^3). This measurement was 39.4 μm of coating thickness for a x standard coating time, 21.9 μm for $0.5x$, 78.8 μm for $2x$ and 118.2 μm for $3x$. The estimated measurement for a standard x coating time (39.4 μm) was quite similar to the coating thickness obtained by scanning electron microscopy (SEM, 40 μm). However, we could not compare the calculated thickness and the SEM results for all the coating levels. In this work, all the coating thickness results are referred to the x standard coating time instead of the microns measurements, in order to simplify and better understand the conclusions.

The uncoated cores had the same API and excipient composition, namely: 35% API and 65% excipients. The excipient mixture contained 40% of excipient #1, 20% of excipient #2, 2% of excipient #3, 1.5% of excipient #4 and 1.5% of excipient #5. The API and the two major excipients in combination accounted for 95% of the tablet content. The presence of the lacquer in the coated tablets reduced the proportions of API and excipients to an extent dependent on the coating thickness. Table 1 shows the resulting changes in the major components.

The samples in groups a and b were used to determine the concentrations of the tablet components (API and excipients).

Table 1 Composition (% w/w) of API and the two major excipients at different coating levels.

Coating level	Sample composition (% w/w)		
	API	E #1	E #2
$0x$	35.0	40.0	20.0
$0.5x$	34.4	39.3	19.7
$1x$	33.9	38.8	19.4
$2x$	33.0	37.7	18.7
$3x$	32.0	36.6	18.3

$0x$ means uncoated core and $1x$ means nominal standard coating.

Those in group *b* were used as calibration and validation sets for the PLS models employed to characterize the coating thickness, which were subsequently applied to the group *c* tablets.

2.2. Instrumentation

Images were acquired with a SyNIRgy^{TM} Chemical Imaging System hyperspectral camera from Malvern Instruments (Malvern, UK). The camera was equipped with an InSb detector with a focal plane array of 320×256 pixels and controlled via the software Pixys$^{\circledR}$ 1.1., also from Malvern. Samples were placed on the plate and lighted with halogen lamps arranged at appropriate angles around the plate, the lens distance being adjusted according to the object size. The images obtained under the selected conditions had a resolution of 40 µm (each pixel covered an area of 40 µm $\times$ 40 µm). The acquisition time for a re ectance image spanning the wavelength range 1200–2400 nm was about 3 min. Prior to acquisition of the image for the sample (*S*), the camera was used to record one for the background (*B*, a reference ceramic plate of 99% re ectance) and another for a dark reference (*D*, a mirror). The image for the sample, S, was converted into re ectance data, *R*, using the equation $R = (S \ D)/(B \ D)$. This calculation was done at every pixel in each image. The data thus obtained were then converted into absorbance units.

Each core was used to record 6 different images: 4 of each outer side (A–D) and 2 of the interior sides (E–F) which were establish by breaking the tablets as shown in Fig. 1a. The analysis of the interior sides was performed to check the homogeneity of the samples. The analytical method does not require breaking the samples as it is considered nondestructive. The tablets group *c* (standard *x* coated) were used to study the four outer sides only, which were designated identically with those of the cores (A–D). On the other hand, each of the two tablets in sample group *b* was used to record the images, one from each of two opposite outer sides. Fig. 1b shows the image of two tablets with identical characteristics (coating thickness). The images were not studied in their entirety, but rather in selected rectangular areas on the inner sides of each tablet in order to avoid image distortions caused by light impinging on tablet edges.
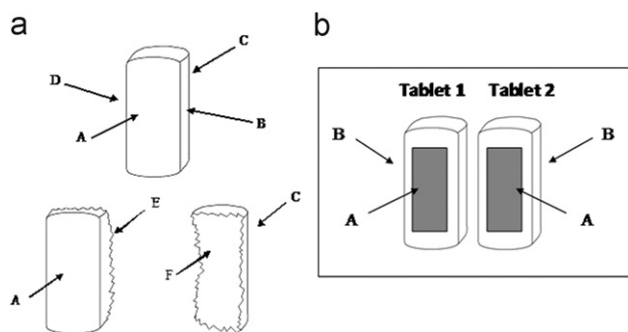

Figure 1 Schema of the tablet sides analyzed by hyperspectral imaging: (a) cores and production tablets and (b) tablets with different coating times. The selected area for analysis of samples (B) is highlighted with dark gray color.

The images for the pure compounds were obtained by placing an adequate powder amount of each in a glass cell and gently pressing its surface prior to recording.

2.3. Data processing

The data in a hyperspectral image are arranged in a three-way data cube $X(M \times N \times \lambda)$ two dimensions in which $(M \times N)$ hold spatial information while the third (λ) contains spectral information.

Prior to application of any spectral treatment or algorithm to extract the required information, the data cube must be unfolded into a two-dimensional matrix since most existing treatments and algorithms have been developed for two-way data. The data matrices thus obtained here from each image were processed with the Standard Normal Variate (SNV) algorithm. All spectral quantitative treatments used were applied using the software Isys 5.0, from Malvern, with routines developed in MATLAB code (MATLAB v 7.0, The MathWorks, Natick, MA). This software only required the previous acquisition of the pure spectrum for each component to be determined [15]. The pure spectra were used to construct a library and then quantify the concentration of each component. The calibration model was completed by selecting an appropriate thresholds and number of factors. Using an increased number of factors increased the variance *Y* explained by the model, but also the risk of overfitting; a compromise was therefore needed for an optimal choice. The threshold used, which allows one to adjust the limits for discrimination between classes, is a function of the similarity between the spectrum for each pure component to be quantified and those for the other components in addition to the number of factors previously selected. Application of the resulting model weighted the spectral data in image based on a 0 to 1 scale. This scale corresponds from 0 to 100% concentration of each component at every pixel of the image. The result was delivered as a concentration map and mean concentration for each component present in the library. This algorithm has been applied for the calculation of the calibration models for every component of the formulation. The information provided by Malvern about the PLS algorithm included in the Isys software is minimum. However we understand this algorithm is a variation of the discriminant PLS, that allows to individually quantify every component of the sample only using its pure spectrum without the need of the other spectra (it does not act as the classical least squares algorithm that strictly needs all the pure spectra components of a formulation).

The thickness and distribution of the coating were quantified using PLS calibration models calculated with the software The Unscrambler v. 9.8 from CAMO (Trondheim, Norway). The PLS regression algorithm [15] uses as *X*-spectral data the mean spectrum of the selected area of every image. The *Y*-variable corresponded to the thickness reference value (Table 1). The PLS model thus constructed was validated by cross-validation applying jack-knifing algorithm in order to identify the wavelength range most strongly correlated with such property. Then, the optimum number of factors was selected under the above-described criteria. The analysis of a NIR-CI image by this PLS model was performed after the unfolding of the three-way data cube into a two-way data set.

The distribution map of tablet coating was performed refolding the two-way data set of PLS prediction results into a three-way data cube.

3. Results and discussion

The goal of this study is the application of NIR-CI to better understand the API and excipients distribution of a novel pharmaceutical formulation and eventually feedback this information to the development stages. Quantitative methods for the determination of tablet components and their distribution in the core and its coating from NIR-CI image have been developed. Fig. 2 shows the spectra for the different pure components of the studied pharmaceutical (viz. the API and 5 excipients). The spectra exhibited marked differences that are confirmed by the pairwise correlation coefficients shown in Table 2. The high spectral similarity of the excipients #2 and #4 (correlation coefficient of 0.984) is one of the main difficulties during the development of the calibration models of these two components. The coating film does not provide a significant absorption compared to the cores spectra. Fig. 3 compares the average spectra of selected area of an uncoated core and a coated tablet. The spectral differences were minimal as a result of the subtle contribution of the coating
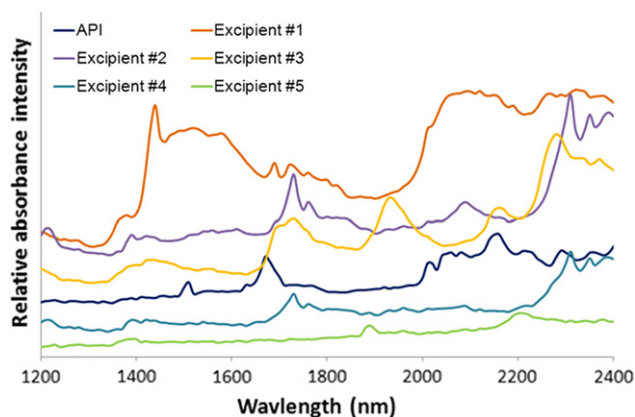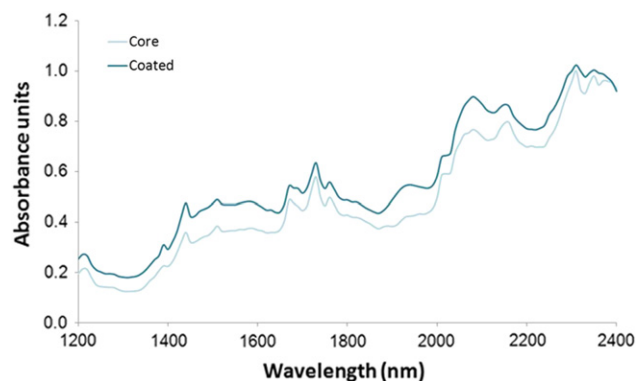

Figure 3 NIR spectra of an uncoated core and a coated tablet. The NIR spectra have been obtained averaging the spectra of each pixel of an area of the hyperspectral image.

Table 3 API and excipients concentration (% w/w) from different sides of the same core.

Core side	Core composition (% w/w)						
	API	E #1	E #2	E #3	E #4	E #5	Sum
Side A	35.51	38.93	20.15	1.97	1.48	1.47	**99.51**
Side B	35.45	39.48	21.12	1.98	1.48	1.51	**101.00**
Side C	37.11	38.45	19.69	1.99	1.53	1.53	**100.30**
Side D	37.45	40.38	20.14	1.95	1.53	1.51	**102.96**
Side E	31.61	44.16	18.62	1.95	1.48	1.51	**99.38**
Side F	31.47	43.38	19.31	1.97	1.55	1.53	**99.21**
Mean	**34.78**	**40.79**	**19.84**	**1.97**	**1.51**	**1.51**	**100.40**
St. dev.	**2.62**	**2.41**	**0.85**	**0.02**	**0.03**	**0.02**	**5.95**

Results calculated with the PLS calibration model. Sides A to F according to Fig. 1.

Figure 2 NIR spectra of pure API and excipients. Each spectrum has been baseline shift to avoid overlapping. The NIR spectra have been obtained averaging the spectra of each pixel of an area of the hyperspectral image.

layer and the lacquer produces a slightly increased baseline of the average spectrum.

3.1. Quantitation of the API and excipients

We constructed a model to determine the concentration of the active principle and five excipients present in the cores by calculating a PLS calibration model for each analyte. The models were constructed by compiling a library containing the spectra for the pure components to be quantified and applying the Isys 5.0 algorithm with a variable number of factors from 3 to 8 depending on the particular analyte. The number of PLS factors needed for each calibration model increases as the concentration of the analyte decreases. The concentrations of the six components thus obtained for each core side are listed in Table 3. The model-predicted concentrations for each core side were very similar to the nominal values for the API and the major and minor excipients. The greatest standard deviation corresponds to the two major components (API and Excipient #1) that indicate an incomplete homogenous distribution. However, the standard deviation for the minor excipients is low, that is a confirmation of their homogeneous distribution. Worth special note is the fact that the combined

Table 2 Correlation coeficient between the average NIR spectra of the pure tablet components (API and excipients).

Correlation coef cients						
	API	E #1	E #2	E #3	E #4	E #5
API	1.000					
E #1	0.810	1.000				
E #2	0.621	0.601	1.000			
E #3	0.693	0.603	0.849	1.000		
E #4	0.640	0.588	0.984	0.903	1.000	
E #5	0.823	0.693	0.669	0.847	0.740	1.000

The NIR spectra have been obtained averaging the spectra of each pixel of the hyperspectral image.

proportions of the components on each side were close to 100% in all cases, which suggest that the calibration models used provide accurate predictions.

However, there are slight differences in composition between sides for the three major components. Thus, the concentrations of the three major components (API and excipients #1 and #2) on the inner sides (E and F) in the cores departed from both the nominal values and the values for the other sides. These differences can be ascribed to the increased roughness of the cut surface, which may in uence the re ectance of the acquired images and consequently it can also in uence the calculated concentrations.

Fig. 4 shows the concentration maps for the components on one of the outer sides of a core as obtained with the Isys 5.0 models. The distributions of excipient #2 and the API were very similar, with coinciding areas of increased concentrations. On the other hand, the high-concentration areas for excipient #1 were complementary with those for the API. This distribution pattern can be ascribed to the fact that the API and excipient #2 are mixed together before the other components are added. By contrast, the minor excipients were uniformly distributed across the images. The API and excipient distributions observed on the other sides and cores exhibited no significant differences from the previous side and exhibited identical patterns.

Fig. 4 also includes the histogram for each core component. The histograms for the minor excipients exhibited a narrow distribution of concentration values. The histograms for the API and excipient #2 were very similarly shaped, with tails on the left. By contrast, the tails in the histogram for excipient #1 were on the right, which suggests an incomplete homogenous distribution of this excipient with the blend of API and excipient #2. In any case, the distributions cannot be considered as normal shaped.

3.2.   Quantitation of coated tablets

The API and excipients were also determined in tablets coated with a lacquer film of variable thickness. We used PLS models
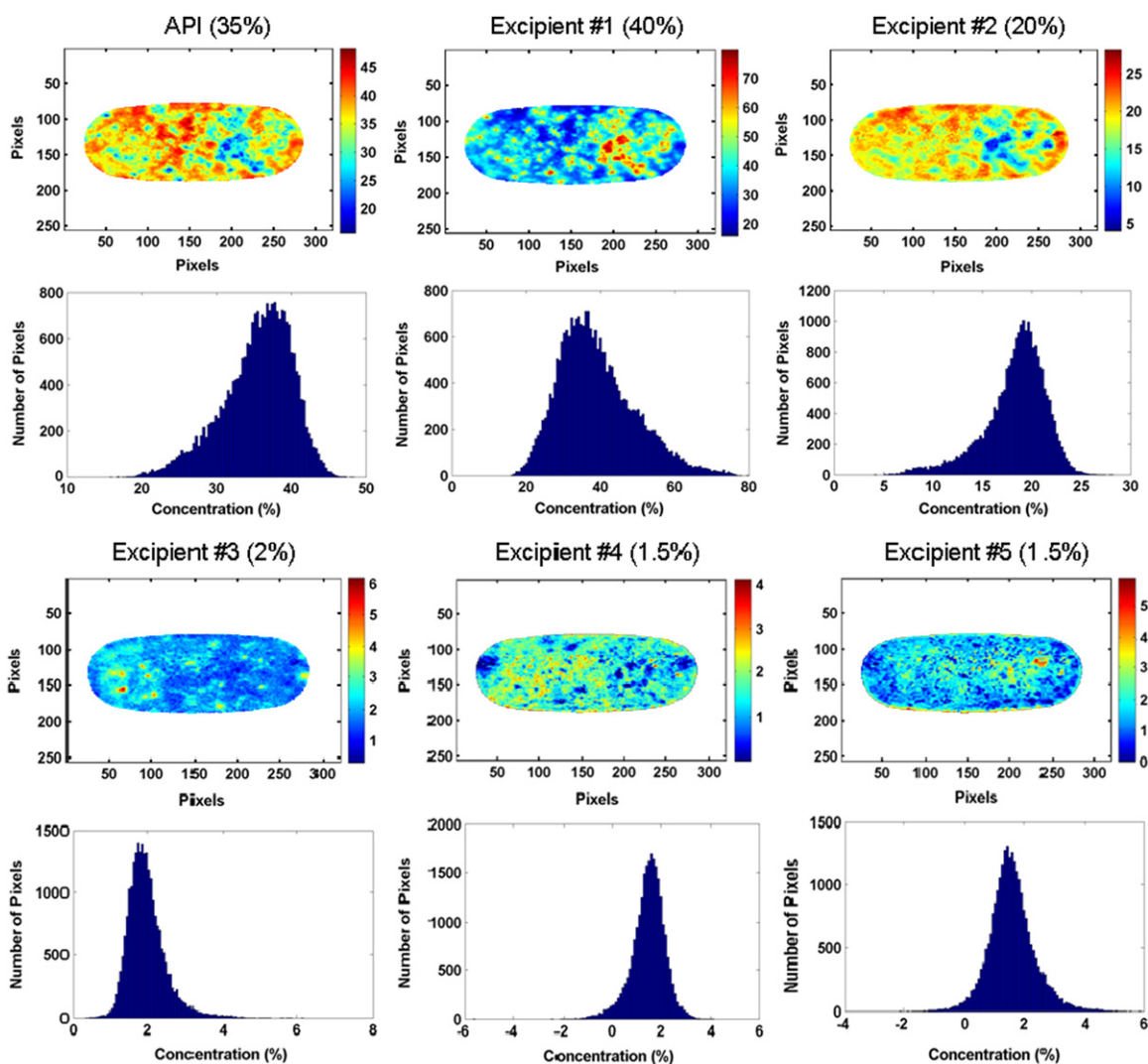

Figure 4   Concentration distribution maps and histograms for API and excipients for side A of a core calculated by PLS. In parenthesis is shown the nominal concentration (% w/w) of each component.

Table 4 Concentrations (% w/w) of API and two major excipients in tablets with different coating thickness.

Coating level	Tablet side	Tablet components (%w/w)		
		API	E #1	E #2
0x	A	35.25	40.74	20.20
	B	35.67	39.46	21.34
0.5x	A	35.85	40.30	19.67
	B	35.31	40.27	20.36
1x	A	34.56	40.80	20.79
	B	35.20	40.18	21.64
2x	A	33.15	39.15	17.95
	B	32.95	42.40	15.31
3x	A	30.85	38.51	12.65
	B	29.65	39.78	14.03

Results obtained with the PLS calibration model.

Figure 5 NIR spectra of tablets coated at different levels. The level $1x$ corresponds to the coating thickness of production tablets.
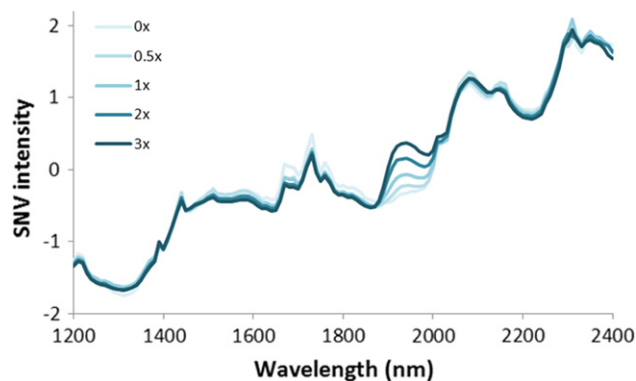
based on an also variable number of factors (3–6) depending on the particular analyte and coating thickness. Table 4 shows the results obtained for two sides (A and B) of the same tablet but coated to a different thickness with a lacquer film. The results are the averages for two tablets coated with an identical coating time and recorded in a single image. The values for the minor components have been omitted because they exhibited high deviations (50–30%) from the nominal values. The calculated concentrations for the three major components are close to their respective nominal values (Table 1) and decrease gradually with increasing coating thickness. Obviously, deviations from the nominal values are the highest in the tablets with the thickest coatings (levels $2x$ and $3x$); this is particularly so for excipient #2, which has the low concentration.

Based on the previous results, the deviations in the calculated concentrations are mainly the result of the lacquer coating, which affects the determination of the concentrations of the major components and, especially, the minor ones. This fact can be related with a higher absorption of the incident radiation or a certain reflective scattering of the coating that reduces the signal of the core components.

3.3. Quantitation of the thickness of coating

The thickness of the coating is an important variable inasmuch as it can influence the rate of dissolution of a tablet and also the quality of components quantitation. In this work, tablet thickness was determined using a PLS model constructed from the average spectrum for each tablet side as a function of coating time. Fig. 5 shows the mean spectra for each coating level (from $0x$ to $3x$). The band between 1800 and 2000 nm increased their intensity with the coating time. Also there are other bands along the whole range that showed differences according to the coating time.

A total of 10 images of tablets coated to a variable thickness (two tablets per image) were obtained. The spectra of the selected area of image were averaged to obtain 4 spectra per each thickness (2 tablets per image and 2 sides per tablet). Three of the 20 spectra thus obtained were discarded as outliers, 12 were used to construct the calibration set and 5 to validate it. Each average spectrum in the calibration set was assigned a time of coating of $0x$, $0.5x$, $1x$, $2x$ or $3x$. These coating thickness were determined from the increase in weight of the tablets upon coating. Different spectral pretreatments were tested during the development of the PLS calibration models (derivation, Savitzky–Golay, SNV) and also different wavelength ranges were selected in order to ensure optimal fitting to the validation set. The best results were obtained by processing data with the SNV algorithm and using the entire spectral range. The calibration model calculated using the spectral range where the coating presented a significant absorption did not improve the predictive ability compared to the model without this range. Under these conditions, a model with a single factor accounted for 99.3% of the total variance. Such a PLS model, which is described in detail in Table 5, was adopted for application to tablets c.

The application of the calibration model to a NIR-CI allowed to quantify the mean coating thickness and its distribution over the surface. Fig. 6 shows the concentration maps for the tablet coating on the four outer sides of a tablet c (Table 1), which were processed with the previous PLS model. A comparison of the four concentration maps reveals that the coating material is not homogenously distributed on all sides. There were some points where the predicted concentration was higher than those on the remainder of the surface. This may have resulted from the formation of lacquer aggregates during the coating process and indicate an irregular spraying inside the coating container drum. Fig. 6 additionally shows the histograms for easier analysis of the heterogeneous coating distribution.

Table 6 shows the average coating values for each of the four studied sides on two tablets c calculated with the above-described PLS model. Both tablet 1 and 2 exhibited differences of up to 10% ($0.1x$) in coating content from the nominal value between sides; however, the average for the four tablet sides was very similar to the nominal value in all samples.
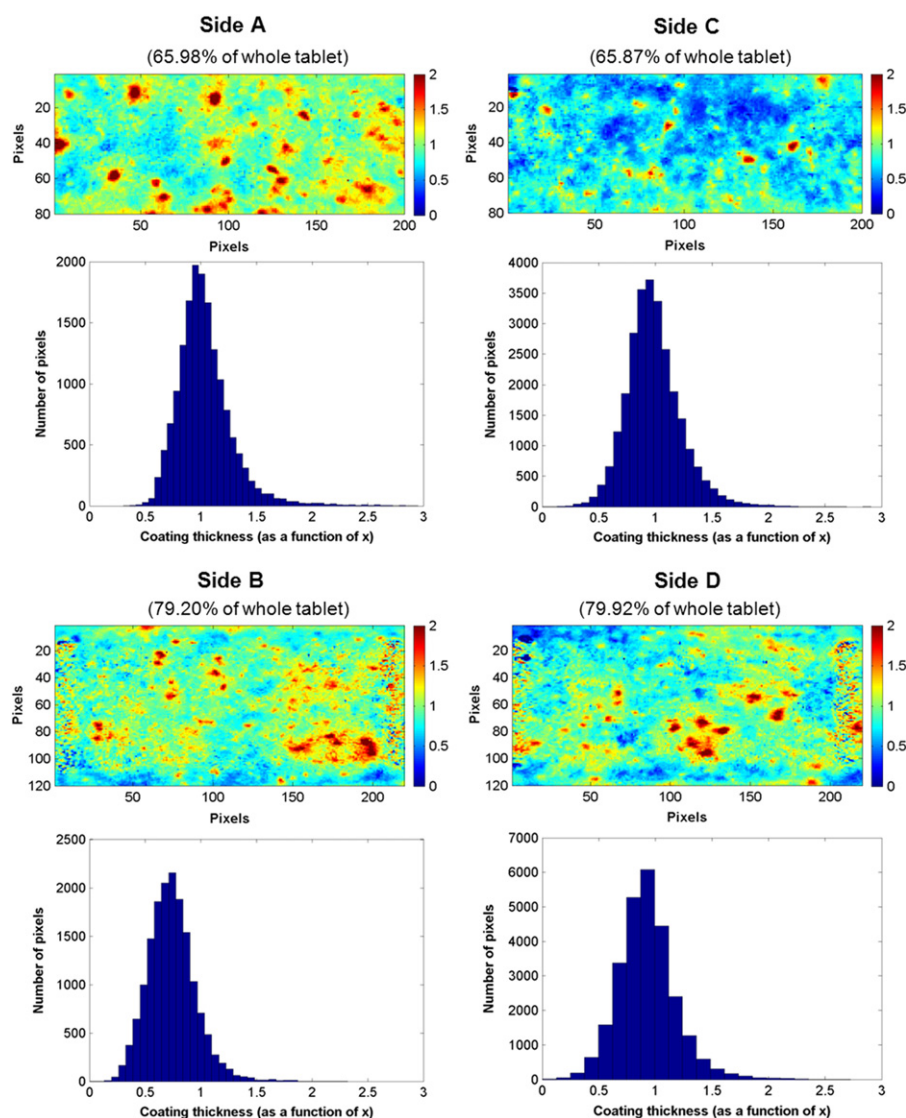
4. Conclusions

In this work, we assessed the potential for the NIR-CI technique for determining the composition of coated and uncoated drug

Table 5   Figures of merit for the quantification of coating thickness obtained with the PLS calibration model.

| PLS calibration model features | | | | | | | |
Number of calibration samples included	Spectral range (nm)	Spectral pretreatment	Number of PLS factors	Y-variance (%)	Number of validation samples	RMSEP[a]	RSEP (%)[a]
12	1200–2400	SNV	1	99.31	5	14.04	8.32

RSEP: Relative Standard Error of Prediction.
[a]RMSEP: Root Mean Square Error of Prediction.

Figure 6   Tablet coating distribution maps and histrograms for the four sides of one production tablet calculated by the PLS calibration model. The percentage of whole tablet image that represents the shown area is provided by the valued between parenthesis.

tablets, and the distribution of their components. We found the PLS algorithm to be effective towards extracting quality quantitative information from hyperspectral images without the need for calibration against reference values, and also towards establishing the distribution of tablet components. Conventional processing of the spectral data contained in an image allows one to determine the thickness of the coating layer with a view to predicting some pharmaceutical properties of the tablet. The expeditiousness with which it allows tablets to be analyzed, and the accuracy of its predictions, make the NIR-CI technique a highly suitable choice for the determination of the quantitative composition of pharmaceutical tablets, and for assessing

Table 6 Coating thickness (as a function of x) in two production tablets obtained applying the described PLS calibration model.

Tablet side	Coating thickness (as a function of x)	
	Tablet 1	Tablet 2
Side A	1.035	1.122
Side B	0.984	1.177
Side C	0.739	1.035
Side D	0.925	1.223
Mean (4 sides)	**0.921**	**1.139**

x = nominal thickness (approximately 40 μm).

uniformity in the distribution of its components and surface coating. These advantages testify to the potential of NIR-CI for use in at-line tests for the control of pharmaceutical production processes.

Acknowledgments

References

[1] A.A. Gowen, C.P. O'Donnell, P.J. Cullen, et al., Recent applications of chemical imaging topharmaceutical process monitoring and quality control, Eur. J. Pharm. Biopharm. 69 (2008) 10–22.

[2] H. Ma, C.A. Anderson, Characterization of pharmaceutical powder blends by NIR chemical imaging, J. Pharm. Sci. 97 (2008) 3305–3320.

[3] W. Li, A. Woldu, R. Kelly, et al., Measurement of drug agglomerates in powder blending simulation samples by near infrared chemical imaging, Int. J. Pharm. 350 (2008) 369–373.

[4] M.B. Lopes, J.C. Wolff, J.M. Bioucas-Dias, et al., Determination of the composition of counterfeit Heptodin tablets by near infrared chemical imaging and classical least squares estimation, Anal. Chim. Acta 641 (2009) 46–51.

[5] J. Cruz, M. Bautista, J.M. Amigo, et al., Nir-chemical imaging study of acetylsalicylic acid in commercial tablets, Talanta 80 (2009) 473–478.

[6] C. Gendrin, Y. Roggo, C. Collet, Content uniformity of pharmaceutical solid dosage forms by near infrared hyperspectral imaging: a feasibility study, Talanta 73 (2007) 733–741.

[7] G. Reich, Near-infrared spectroscopy and imaging: basic principles and pharmaceutical applications, Adv. Drug Delivery Rev. 57 (2005) 1109–1143.

[8] C. Cairós, J.M. Amigo, R. Watt, et al., Implementation of enhanced correlation maps in near infrared chemical images: application in pharmaceutical research, Talanta 79 (2008) 657–664.

[9] L. Maurer, H. Leuenberger, Terahertz pulsed imaging and near infrared imaging to monitor the coating process of pharmaceutical tablets, Int. J. Pharm. 370 (2009) 8–16.

[10] J. Hogan, Diseno y fabricación de las formas farmacéuticas, in: M.E. Aulton (Ed.), Farmacia la ciencia del diseno de las formas farmacéuticas, Elsevier, Madrid, 2004, pp. 441–448.

[11] L. Zhang, M.J. Henson, S. Sonja, Multivariate data analysis for Raman imaging of a model pharmaceutical tablet, Anal. Chim. Acta 545 (2005) 262–278.

[12] J.M. Amigo, J. Cruz, M. Bautista, et al., Study of pharmaceutical samples by NIR chemical image and multivariate analysis, Trends Anal. Chem. 27 (2008) 696–713.

[13] C. Ravn, E. Skibsted, R. Bro, Near-infrared chemical imaging (NIR-CI) on pharmaceutical solid dosage forms—comparing common calibration approaches, J. Pharm. Biomed. Anal. 48 (2008) 554–561.

[14] L.J. Makein, L.H. Kidder, E.N. Lewis, et al., Non-destructive evaluation of manufacturing process changes using near infrared chemical imaging, NIR News 19 (2008) 11–15.

[15] T. Puchert, D. Lochmann, J.C. Menezes, et al., Near-infrared chemical imaging (NIR-CI) for counterfeit drug identification—a four-stage concept with a novel approach of data processing, J. Pharm. Biomed. Anal. 51 (2010) 138–145.